Supporting Information for

Using Geostationary-Derived Sub-Daily FRP Variability vs. Prescribed Diurnal Cycles: Impact of African Fires on Tropospheric Ozone

Haolin Wang[1,2], William Maslanka[3,4,5], Paul I. Palmer[2,6*], Martin J. Wooster[3,4,5], Haofan Wang[1], Fei Yao[2,6], Liang Feng[2,6], Kai Wu[7], Xiao Lu[1*], Shaojia Fan[1*]

[1] School of Atmospheric Sciences, Sun Yat-sen University, and Southern Marine Science and Engineering Guangdong Laboratory (Zhuhai), Zhuhai, China

[2] School of GeoSciences, University of Edinburgh, Edinburgh, UK

[3] Department of Geography, King's College London, London, UK

[4] National Centre for Earth Observation, King's College London, London, UK

[5] Leverhulme Centre for Wildfires, Environment and Society, King's College London, London, UK

[6] National Centre for Earth Observation, University of Edinburgh, Edinburgh, UK

[7] Department of Civil and Environmental Engineering, University of California, Irvine, CA, USA

*To whom correspondence should be addressed.

Email: pip@ed.ac.uk (Paul I. Palmer), luxiao25@mail.sysu.edu.cn (Xiao Lu), and eesfsj@mail.sysu.edu.cn (Shaojia Fan)

This PDF file includes:

Supporting Table S1 and Figs. S1 to S10

Table S1. Spatial correlation and mean bias (in the brackets) between observations and simulations (unit: DU for CO and O_3, and 10^{16} molecules cm^{-2} for NO_2).

	Month	GFED4_3hourly	GFAS_daily	FREM_hourly	FREM_3hourly	FREM_daily
CO	Jan	0.91 (1.47)	0.89 (0.13)	0.90 (2.10)	0.90 (2.11)	0.90 (2.11)
	Apr	0.92 (-3.92)	0.92 (-3.41)	0.92 (-3.86)	0.92 (-3.87)	0.92 (-3.89)
	Jul	0.95 (5.97)	0.90 (1.56)	0.94 (6.41)	0.94 (6.32)	0.93 (6.25)
	Oct	0.58 (5.42)	0.52 (5.34)	0.49 (4.82)	0.49 (4.81)	0.49 (4.82)
NO_2	Jan	0.79 (0.04)	0.82 (0.01)	0.81 (0.02)	0.81 (0.02)	0.79 (0.03)
	Apr	0.84 (0.01)	0.84 (0.01)	0.83 (0.01)	0.83 (0.01)	0.83 (0.01)
	Jul	0.87 (0.08)	0.90 (0.02)	0.89 (0.06)	0.90 (0.05)	0.89 (0.05)
	Oct	0.78 (0.01)	0.82 (-0.0004)	0.84 (-0.002)	0.84 (-0.003)	0.83 (-0.002)
TROPOMI O_3	Jan	0.54 (-1.05)	0.62 (-2.84)	0.60 (-0.50)	0.60 (-0.50)	0.60 (-0.53)
	Apr	-0.28 (-4.33)	-0.28 (-4.55)	-0.29 (-1.59)	-0.29 (-1.58)	-0.29 (-1.58)
	Jul	-0.03 (1.71)	-0.10 (-0.59)	-0.07 (0.04)	-0.07 (0.06)	-0.06 (0.04)
	Oct	0.80 (-2.44)	0.77 (-3.01)	0.78 (-1.84)	0.78 (-1.84)	0.78 (-1.86)
OMI O_3	Jan	0.77 (9.17)	0.81 (7.92)	0.80 (8.13)	0.80 (8.15)	0.80 (8.15)
	Apr	0.87 (3.10)	0.88 (2.93)	0.87 (2.89)	0.87 (2.90)	0.87 (2.89)
	Jul	0.72 (4.14)	0.85 (2.81)	0.84 (3.02)	0.83 (3.03)	0.83 (3.03)
	Oct	0.92 (2.26)	0.93 (1.86)	0.94 (1.78)	0.94 (1.79)	0.94 (1.78)

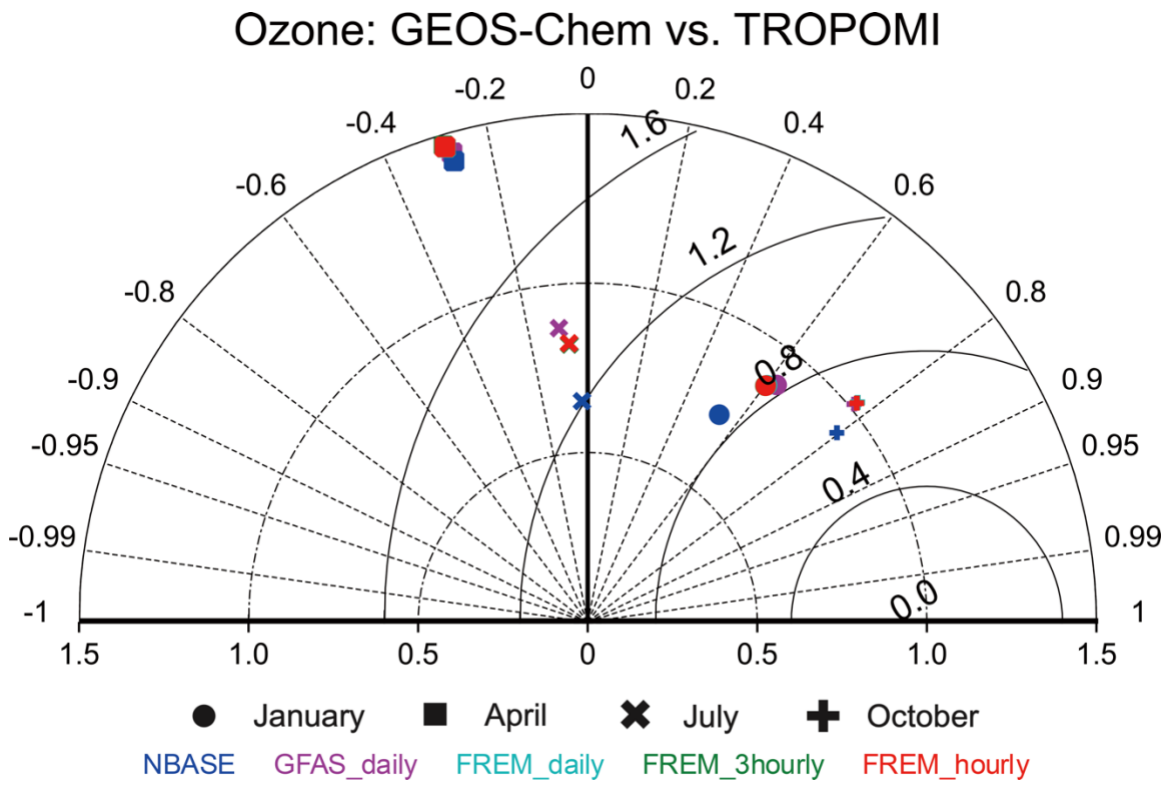

Figure S1. Same with Figure 2, but for TROPOMI tropospheric ozone column.

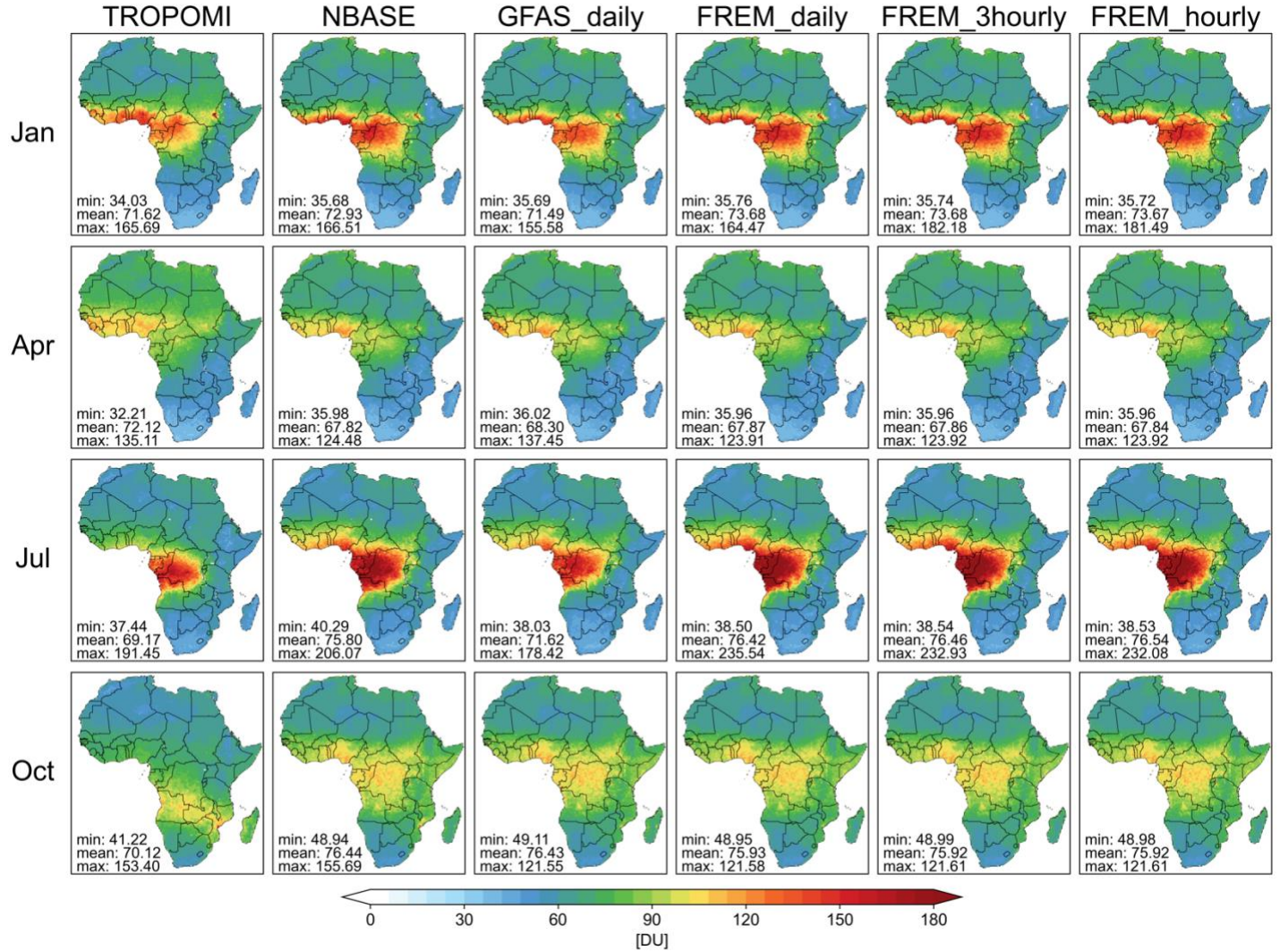

Figure S2. Comparison of TROPOMI CO total column with modelled results with different biomass burning emission inventories.

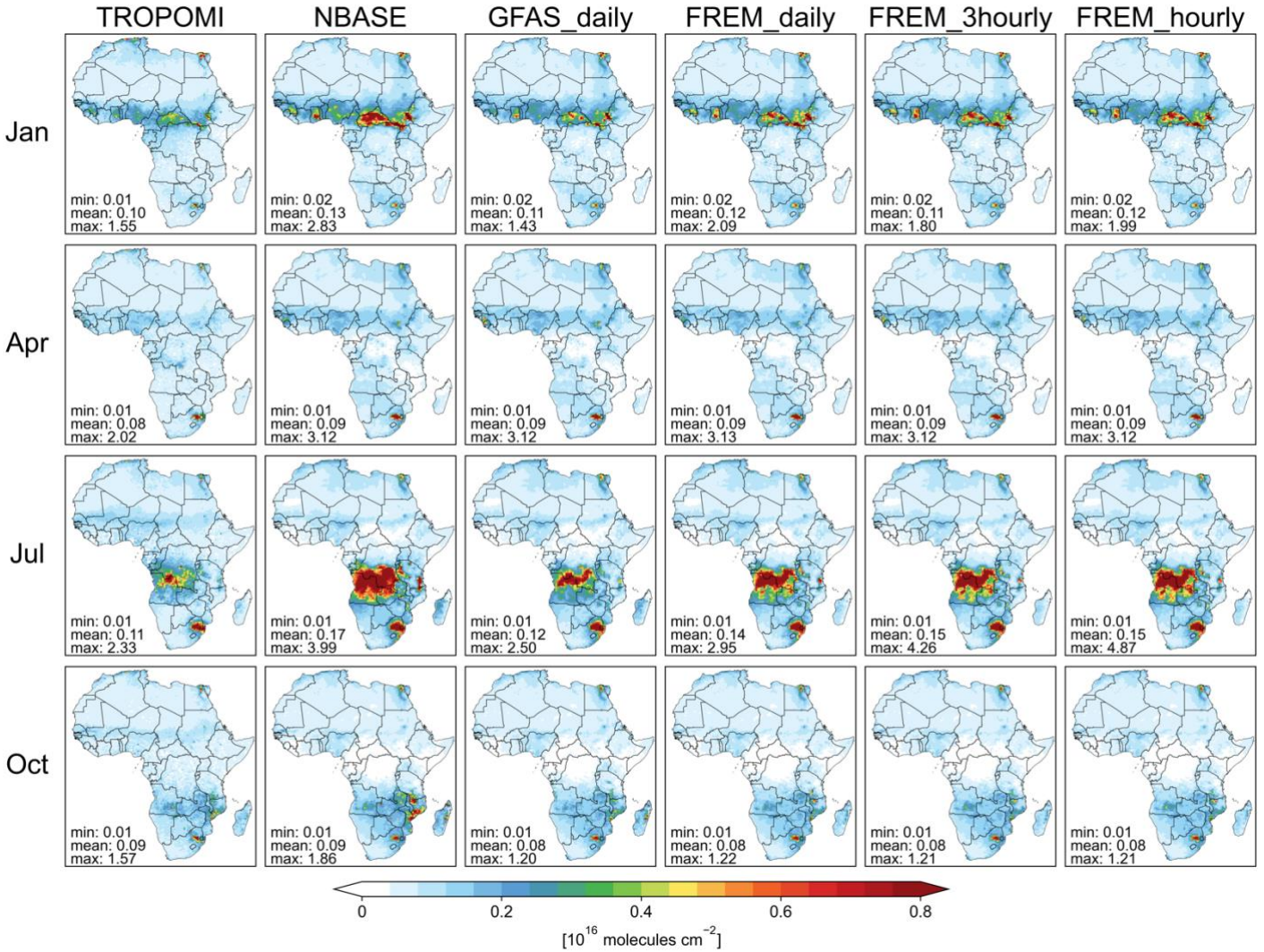

Figure S3. Same with Figure S2, but for tropospheric NO_2 column.

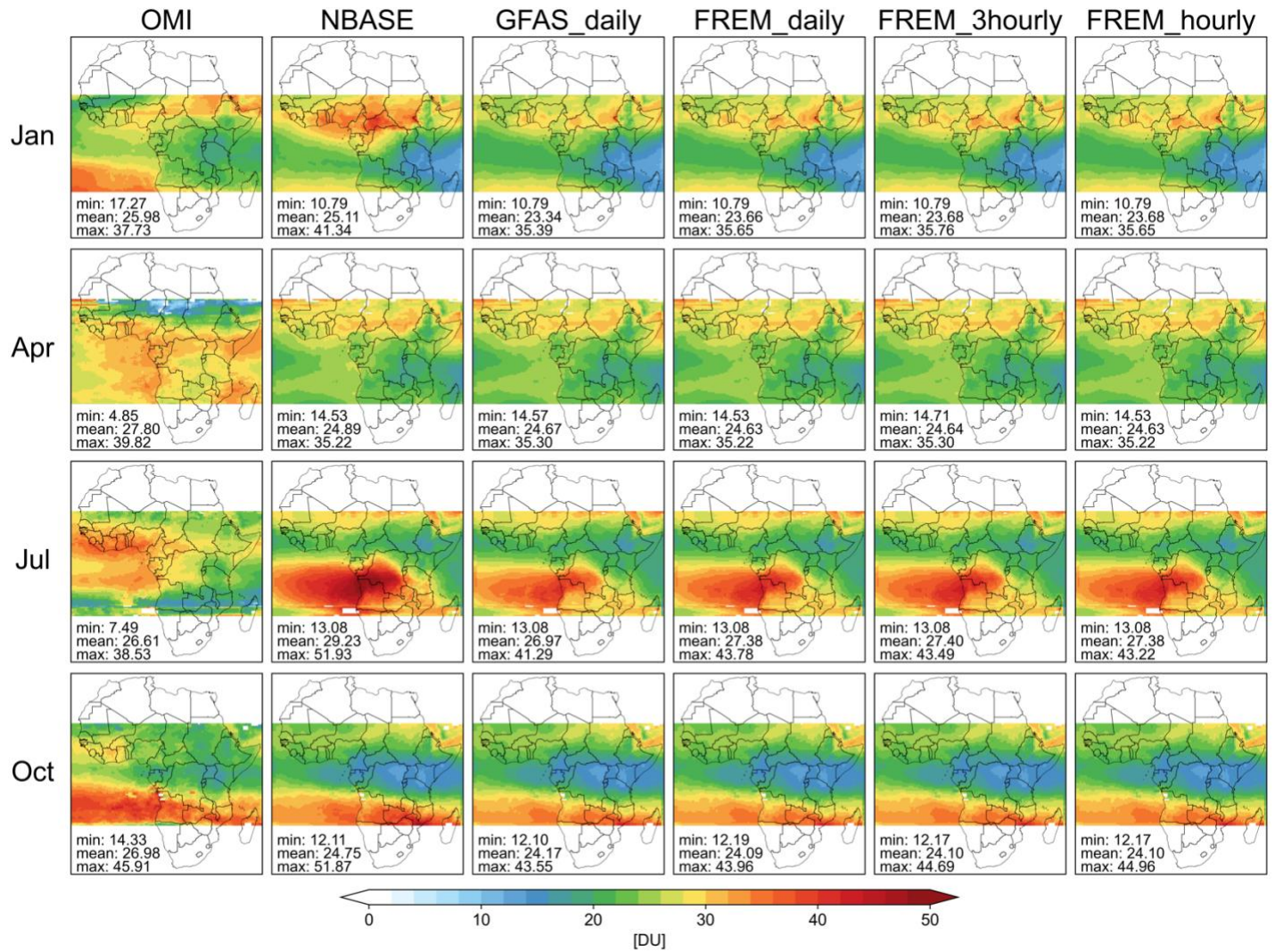

Figure S4. Same with Figure S2, but for TROPOMI tropospheric ozone column.

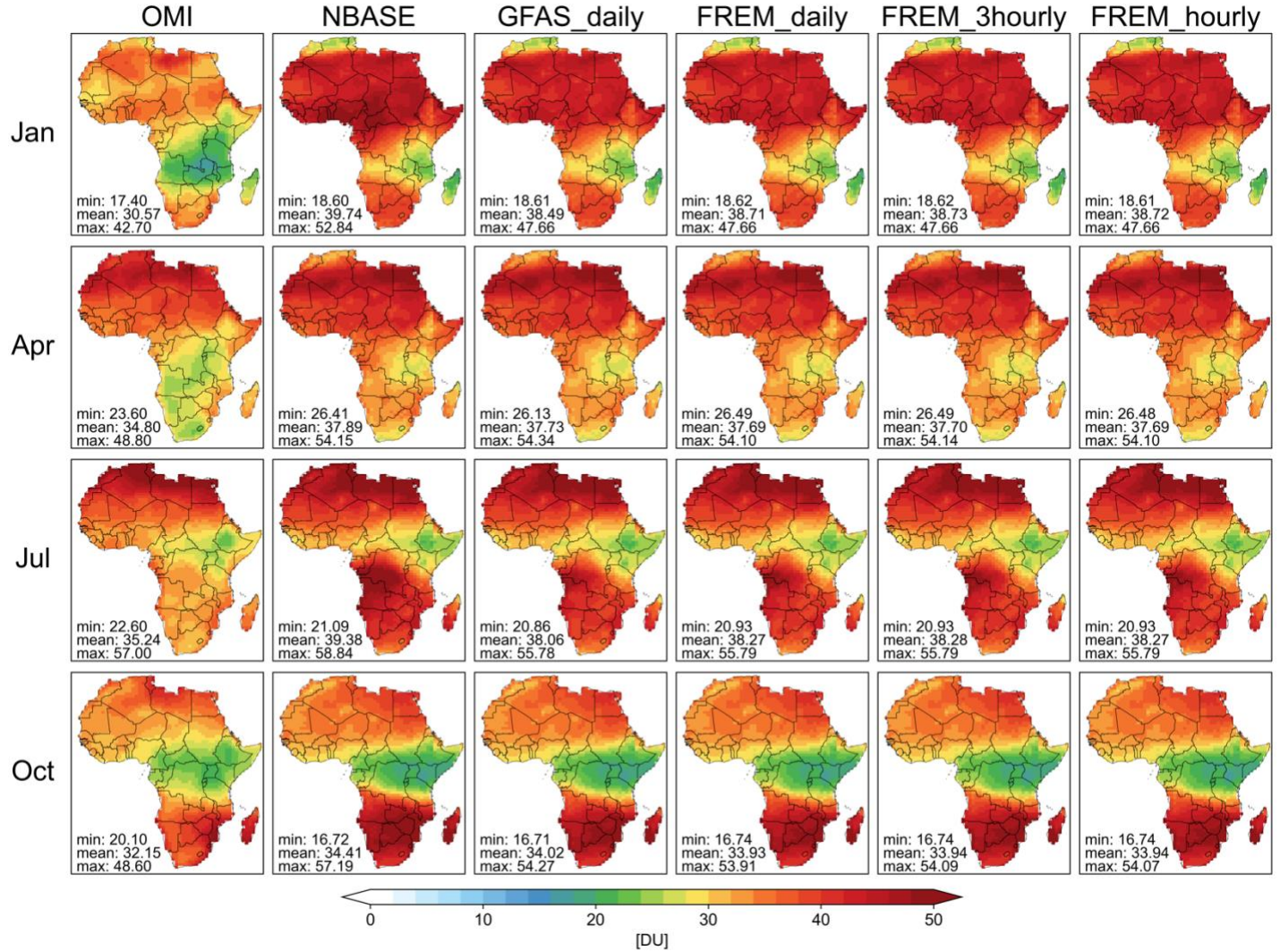

Figure S5. Same with Figure S4, but for OMI tropospheric ozone column.

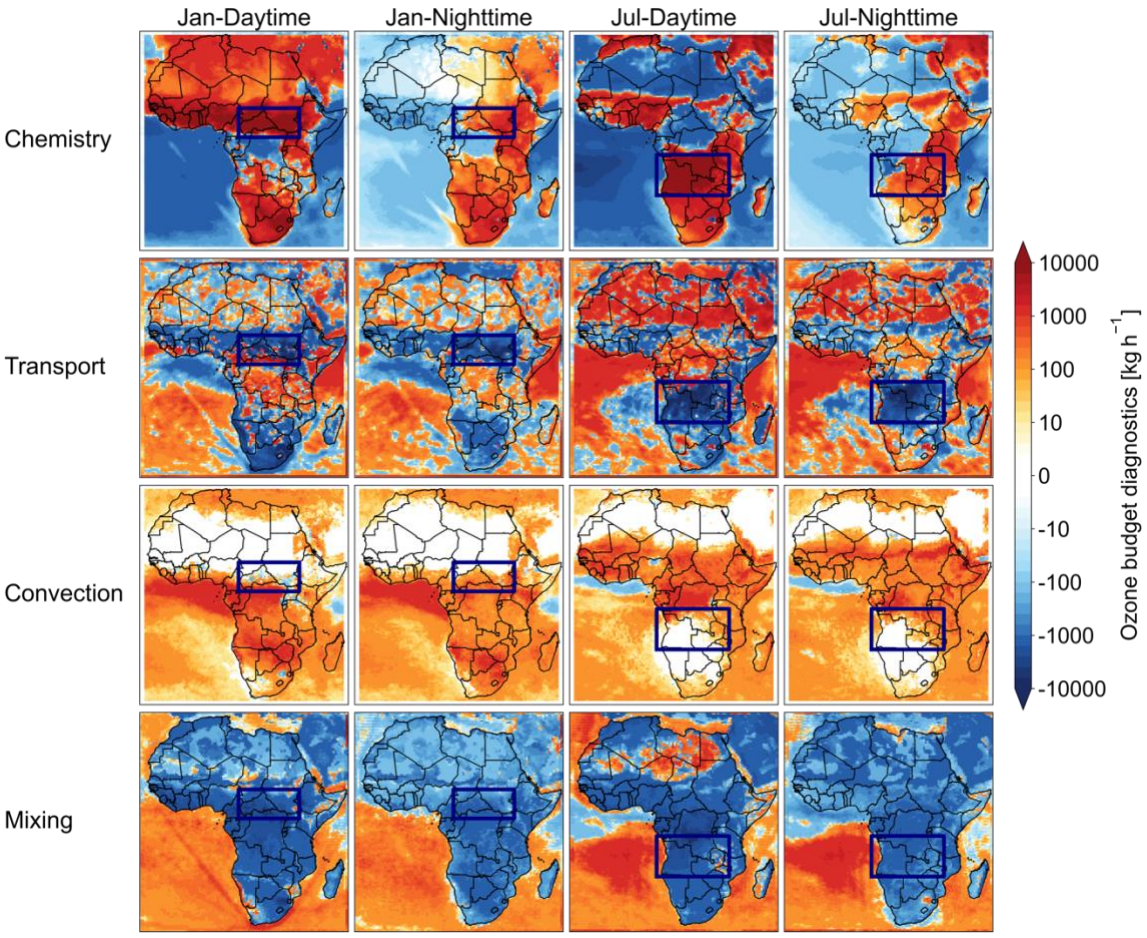

Figure S6. Ozone budget diagnostics (kg h^{-1}) in Africa for January and July 2019 from FREM_hourly, as estimated by the GEOS-Chem model. The diagnostics include contributions from chemistry, transport, convection, and mixing, with results shown separately for daytime and nighttime in each month.

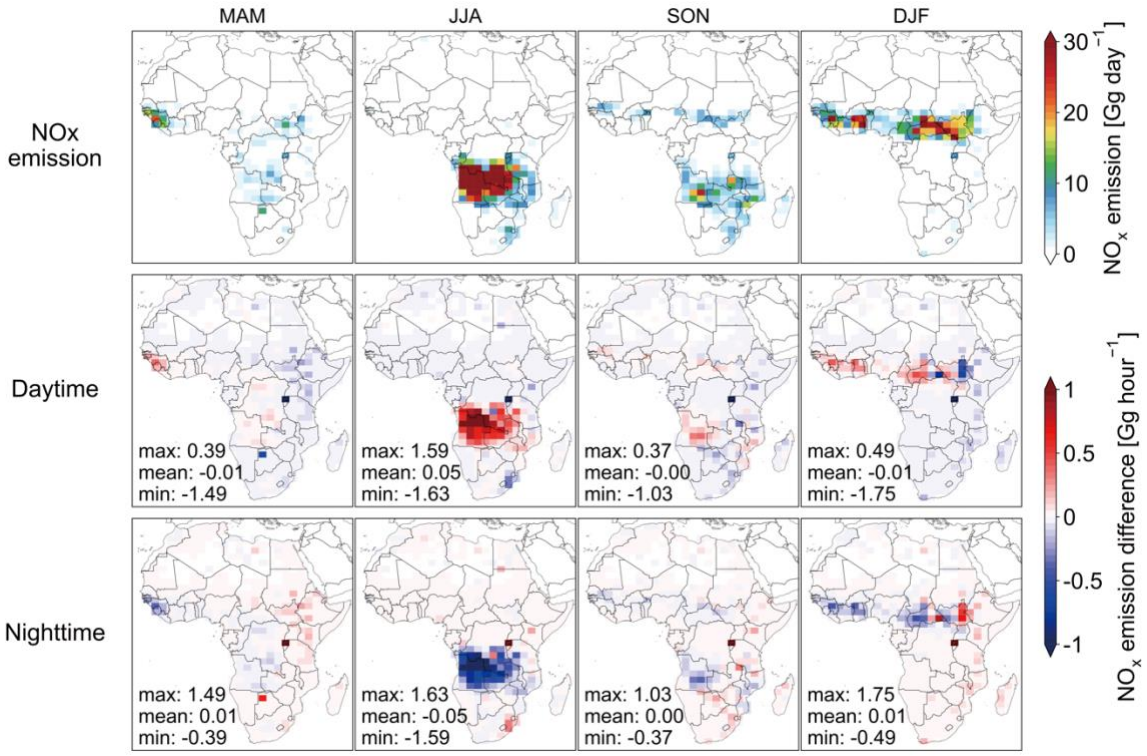

Figure S7. Spatial distribution of biomass burning NO_x emissions and daytime and nighttime differences between FREM hourly and FREM daily biomass burning emissions for different seasons in 2019.

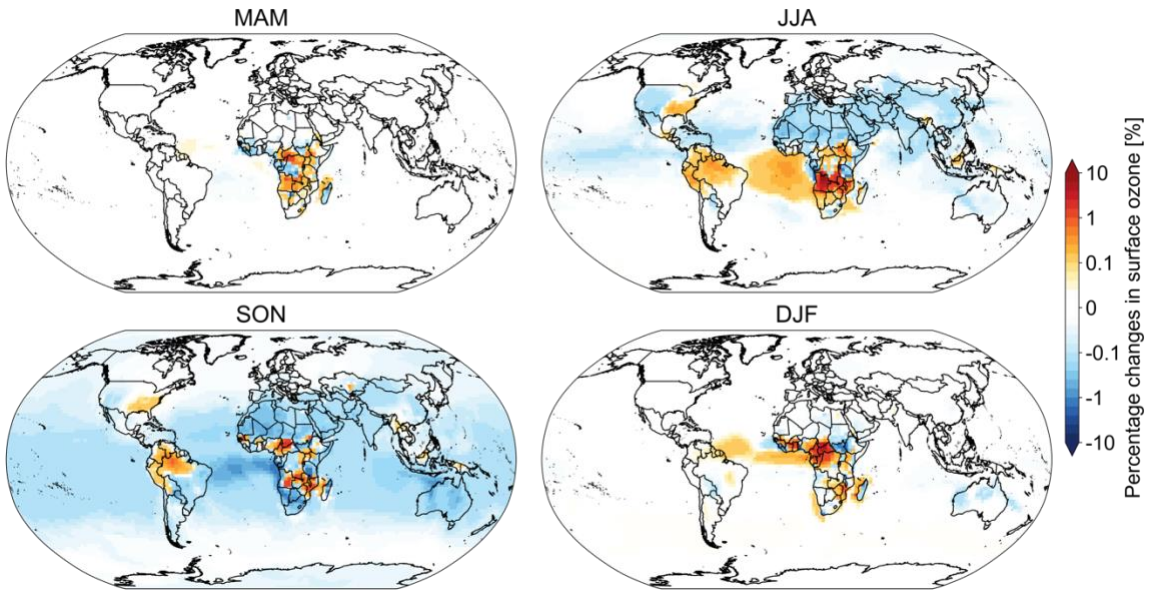

Figure S8. Same as Figure 5, but for the relative change in surface ozone.

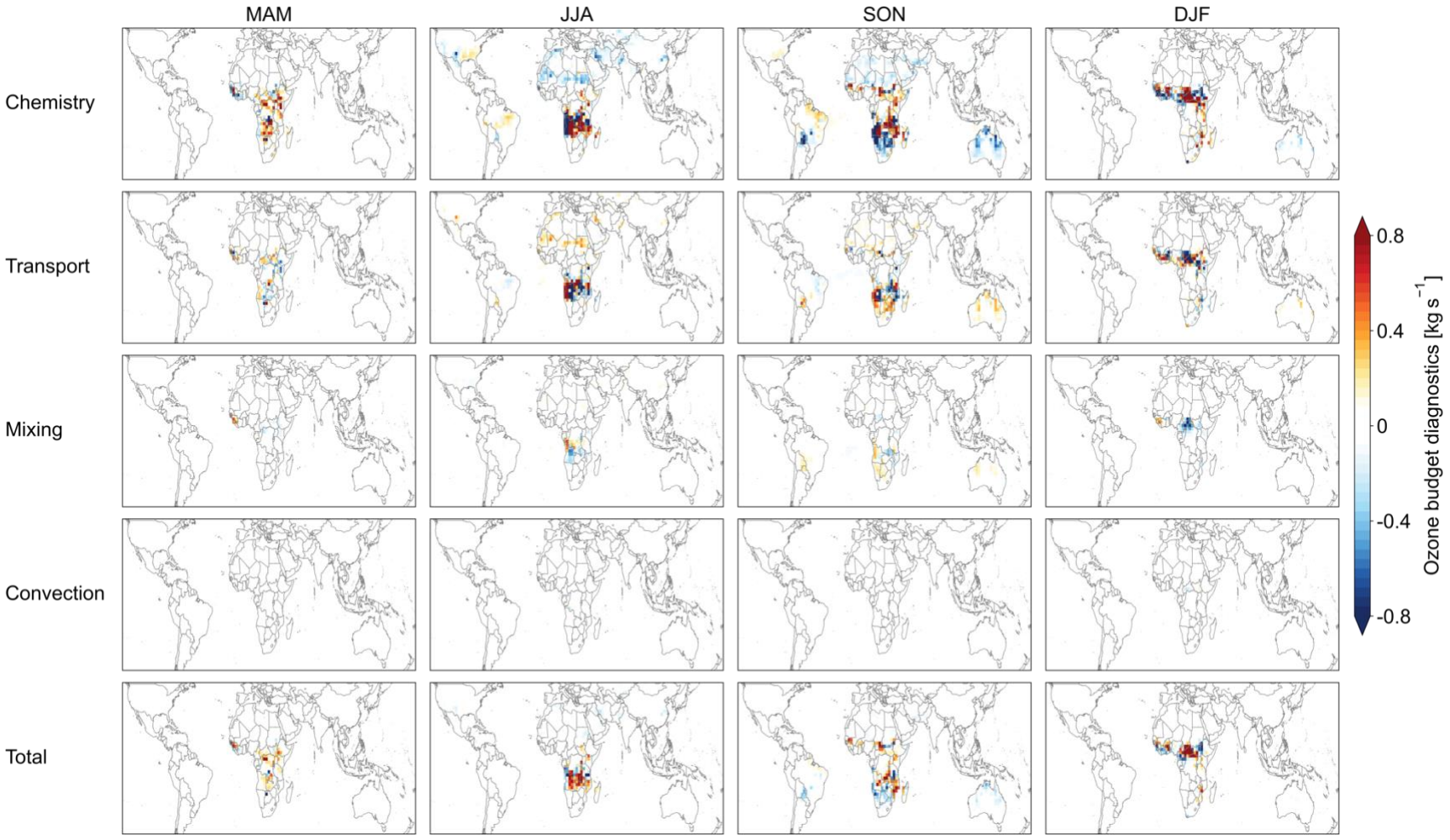

Figure S9. The impact of diurnal variations in African biomass burning emissions on ozone budget diagnostics (kg s^{-1}) across different seasons in 2019, estimated using the GEOS-Chem model, includes effects from chemistry, transport, mixing, and convection.

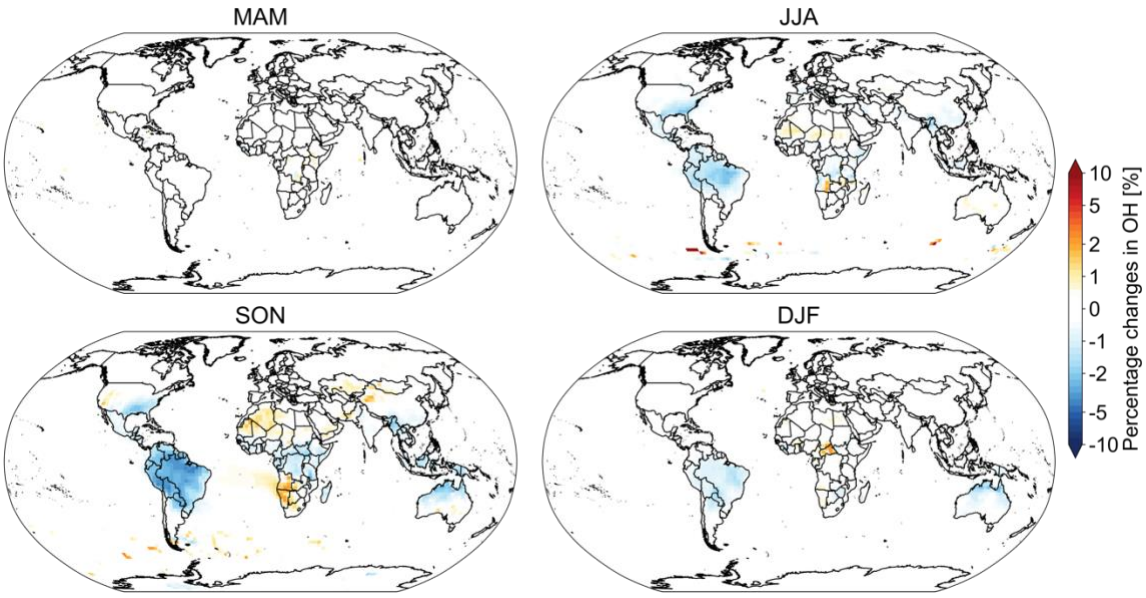

Figure S10. Same as Figure 5, but for the relative change in OH.